1. VFS and BFS flow dividers

Passive flow dividers were used to collect water samples from the VFS and BFS drains. These flow dividers were essentially open tubes attached to a supporting frame, which collected a portion of the volume of each bucket tip. In the VFS manhole, flexible, Teflon-coated tubes were attached to rigid tubes, cut so as to be open on top (metal rigid tubes emptied into glass bottles and plastic rigid tubes emptied into plastic bottles), enabling the collection of 3% of the water flow per tube (Figure S1a). In the BFS manhole, Teflon-coated tubes were attached directly to the supporting frame (Figure S1b). This system collected about 1% of water flow per tube.

(a) (b)

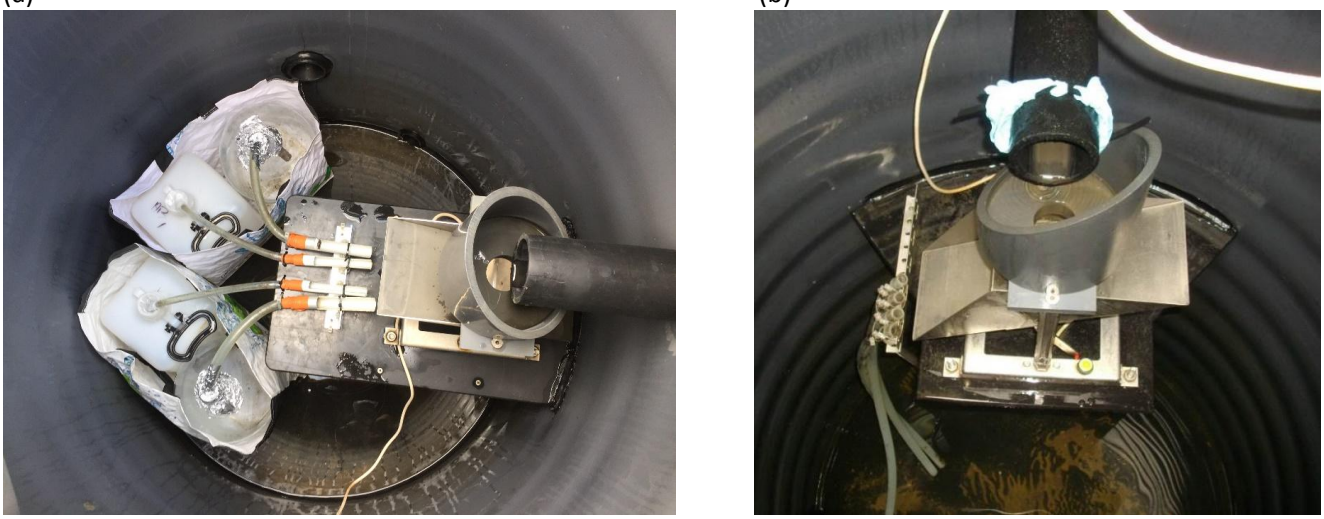

Figure S1 : Passive flow dividing sampling systems

2. Field Blanks

2.1. Methodology

Field blanks were carried out to verify the non-contamination of samples from the RR automatic sampler and associated tubing, a PVC pipe at the inlet of the RR manhole and water collection system in the VFS manhole and associated tubing, which was assumed to be representative of the similar BFS system. Blanks were conducted for metals, major elements and organic micropollutants.

As no running water was available on site and large volumes of water were required, tap water stored in identical, plastic buckets were used. The buckets were cleaned with TDF-4 detergent and rinsed multiple times with tap water and followed by deionized water prior to use. A reference sample, representative of the initial water quality, was taken of the water stored in these buckets.

Each piece of equipment was rinsed thoroughly with water from the buckets before production of the blank samples. Water for each sample (including the reference) was manipulated with the same plastic beaker.

For the RR automatic sampler, blanks were taken twice. The first time, the automatic sampler and the PVC pipe were tested separately. For the automatic sampler, water was placed in the beaker and the peristaltic pump of the sampler activated to pump water into a sampling bottle. In the PVC pipe, for the initial campaign, water was left to stagnate 4h, a largely pessimistic duration. For pollutants that were not released after such a long stagnation, it was concluded that they would not be released for the shorter residence times representative of real operation. However, as large increases in phthalate concentrations were observed, a second campaign was conducted under more realistic conditions. For this second campaign, the residence time was calculated using the average flow rate in the pipe and its volume. The residence time was found to be 12s, which was rounded up to 1 minute for logistic purposes. This time, the pipe was filled and water pumped from it using the automatic sampler while continuously adding water from the bucket at a rate ensuring the required residence time.

In VFS, water was poured into the tipping bucket and collected at the outlet of tubing in a field sampling bottle.

Blanks were only analyzed for the dissolved phase of pollutants. Table S1 presents the results of these campaigns. Results are presented as the ratio of the change in concentration between each blank and the reference divided by the median dissolved concentration in the water from the sampling point. The analytical uncertainty in the change in concentration was taken into account: ratios marked with a star are analytically significantly superior to zero.

2.2. Blank Results

The grand majority of pollutants showed no significant contamination by sampling equipment. At RR, a slight contamination, equivalent to 5-13% of median dissolved concentrations in RR water was observed for As, Cu, V, Zn and NP1EC. Mo concentrations increased by 67% of observed concentrations.

The concentrations of several PAH molecules (NAP, 1MN, 2MN, F and P) were much greater in the VFS blank than the reference. However, as dissolved concentrations of all of these molecules were nearly always below the LOQ at the VFS outlet, these observations do not appear to be representative of the true behavior of the system. As these molecules were quantified in the reference water for the blank, the contamination more likely comes from the plastic buckets. The VFS blank was not repeated in response to this result as even if some contamination were occurring, it was unmeasurable during real sampling campaigns and would not, therefore, bias interpretation. No other analytically significant contamination occurred in the VFS blank.

As previously mentioned, the first series of blanks showed significant contamination of all phthalate molecules from the PVC pipe. As PVC is known to contain phthalates and water was left to stagnate for a long period, it is unsurprising that some contamination was observed. The second campaign, conducted in more realistic conditions with a residence time of only one minute, showed no contamination. It is therefore concluded that, under real operation conditions, contamination by phthalates at RR is not a problem.

	RR Automatic Sampler Blank	RR PVC Pipe Blank (Residence time : 4h)	RR PVC Pipe + Automatic Sampler Blank (Residence time: 1 minute)	VFS Blank
Al (mg/L)	0	0	-	0
Fe (mg/L)	0	0	-	0
Mn (mg/L)	0	0.67*	-	0
Mo (mg/L)	0	0	-	0
Sr (mg/L)	0.02	0	-	0
Ti (mg/L)	0	0	-	0
Na (mg/L)	0	0	-	0
K (mg/L)	0	0.08	-	0
Mg (mg/L)	0.03	0	-	0
Ca (mg/L)	0.02	0.01	-	0.01
Ba (mg/L)	0	0	-	0
Si (mg/L)	0.02	0	-	0
As (µg/L)	0	0.05*	-	0
Cd (µg/L)	0	0	-	0
Co (µg/L)	0	0	-	0
Cr (µg/L)	0	0	-	0
Cu (µg/L)	0.1*	0.01	-	0
Ni (µg/L)	0	0	-	0
Pb (µg/L)	0	0	-	0
V (µg/L)	0.01	0.13*	-	0
Zn (µg/L)	0.06*	0.11*	-	0
TPH (mg/L)	0	0	-	0
Nap (ng/L)	0	0	-	1.6
1MN (ng/L)	0	0	-	0.6
2MN (ng/L)	0	0	-	0.4
Acyl (ng/L)	0	0	-	0
Acen (ng/L)	0	0	-	0
F (ng/L)	0	0	-	10.7*
A (ng/L)	0	0	-	0

P (ng/L)	0	0	-	9.8*
Fluo (ng/L)	0	0	-	0
Pyr (ng/L)	0	0	-	0
BaA (ng/L)	0	0	-	0
Chry (ng/L)	0	0	-	0
BaP (ng/L)	0	0	-	0
BbF (ng/L)	0	0	-	0
DahA (ng/L)	0	0	-	0
BkF (ng/L)	0	0	-	0
BPer (ng/L)	0	0	-	0
IP (ng/L)	0	0	-	0
Cor (ng/L)	0	0	-	0
BPA (ng/L)	0	0	-	0
NP1EC (ng/L)	0	0.06*	-	0
OP (ng/L)	0	0	-	0
OP1EO (ng/L)	0	0	-	0
OP2EO (ng/L)	0	0	-	0
4-NP (ng/L)	0	0.05	-	0
NP1EO (ng/L)	0	0	-	0
NP2EO (ng/L)	0	0	-	0
DMP (ng/L)	0	6.1*	0	0
DiBP (ng/L)	0	84*	0	0
DBP (ng/L)	0	12*	0	0
DEHP (ng/L)	0	1.6*	0	0.07
DNP (ng/L)	0	2.1*	0	0

Table S1: Ratio of concentration increase in field blank to median dissolved concentration from sampling campaigns. *Indicates the analytical significance of the concentration increase

3. Sampling Efficiency

At RR, a 250 mL sample was collected every 10th bucket tip, up to 80 samples per event. The mean time between samples was 6 minutes. Continuous turbidity measurements showed that the average turbidity of RR samples (the average of turbidity each minute that samples were taken) were an average of ±13% from the average flow-weighted turbidity for the full event. In the BFS, the mean time between samples was 4.6 minutes; in the VFS, it was 1.2 minutes. Although no continuous turbidity measurements were available at these points, a part of the flow was collected every second bucket tip (or every second liter), so even rapid changes in concentration have likely been taken into account in mean samples.

The methodology aimed to collect mean samples for each sampling period. In order to evaluate the efficiency of sampling, the fraction of total event volume covered by the collected sample was calculated for all sampled rain events. For this calculation, runoff events were defined as beginning with the first rainfall record and ending when all flows (RR, VFS drain and BFS drain) became negligible (flow less than 0.5% of the accumulated event volume over the last hour). Each sampling period included between 1-4 runoff events (usually with one dominant event).

Efficiency was 100% if the sample was collected over the full length of the event. Sampling efficiencies less than 100% occurred when (1) sampling equipment was installed when it was already raining, (2) when sampling bottles were full before the end of the event or (3) when the sample was collected before flow had completely finished.

VFS event coverage was often poor (median 34%, Table 3) as geometric constraints in the manhole required smaller sampling bottles (10L rather than 20L) which often overflowed. As pollutographs issued from previous studies have shown outlet concentrations of TSS and metals for biofiltration systems to be higher towards the beginning of events (Hatt et al., 2009), event mean concentrations for the VFS may tend to be slightly overestimated and the efficiency of treatment underestimated.

	Median (min, max)
% Event Volume Represented by RR Sample	96 (64, 100)
% Event Volume Represented by BFS Sample	93 (33, 100)
% Event Volume Represented by VFS Sample	34 (10, 100)

Table S2: Sampled rain event characteristics

4. Uncertainty Calculations

Uncertainty was evaluated for total and dissolved concentrations according to the methods established in each laboratory effectuating the analysis. The methods used by laboratories to evaluate uncertainties were variable. As such, as well as the structure of the errors (relative or absolute uncertainties in different ranges) were variable, the levels of confidence associated with the uncertainty intervals depended upon the species. The evaluation of uncertainties of more commonly analyzed parameters, such as trace and major elements, nutrients and PAHs were established using inter-laboratory comparisons according to the norms NF ISO 11352 ou NF T90-200. The uncertainties of BPA, alkylphenols and phthalates were evaluated based on a 5 repetitions of a single analysis and a lower level of confidence (80%) was used.

When particulate and dissolved concentrations were measured, total concentration uncertainty was calculated according to Equation S1, which supposes that analytical errors are independent.

$$\delta_{C_T} = \sqrt{\left(\delta_{C_D}\right)^2 + \left(\delta_{C_{TSS}} \cdot C_P\right)^2 + \left(\delta_{C_P} \cdot C_{TSS}\right)^2} \qquad \text{(Eq. S1)}$$

where $\delta_{C_T}, \delta_{C_D}, \delta_{C_{TSS}}$ and δ_{C_P} are the absolute uncertainties of the total concentration (ng/L), dissolved concentration (ng/L), TSS concentration (mg/L) and particulate concentration (ng/mg), respectively, C_p is the particulate concentration for the pollutant in ng/mg and C_{TSS} is the TSS concentration (mg/L).

Uncertainty was then propagated to the E_c calculation according to Equation S2, derived assuming inlet and outlet errors to be independent.

$$\delta_{E_C} = 100\sqrt{\left(\delta_{C_{RR}} \cdot \frac{C_{outlet}}{C_{RR}^2}\right)^2 + \left(\delta_{C_{outlet}} \cdot \frac{-1}{C_{RR}}\right)^2} \qquad \text{(Eq. S2)}$$

where $\delta_{E_C}, \delta_{C_{RR}}, \delta_{C_{outlet}}$ are the absolute uncertainties associated with the concentration reduction (%), RR and outlet concentrations (units of concentration, depending on the pollutant), respectively.

5. Global parameters in road runoff

R had a relatively stable and slightly alkaline pH (median 8.02, Table 4). EC was found to be highly variable (88-1950 µS/cm), with peaks occurring following NaCl salt application on the road surface in winter.

TP, TKN and N-NO_3^- median concentrations (2.92, 0.48, and 0.47 mg/L, respectively) were consistent with results reported by Kayhanian et al. (2012), while N-NH_4^+ concentrations (median 0.2 mg/L) were relatively low. Objective concentrations (MEEM, 2016) were surpassed frequently for TP, occasionally for nitrite and ammonium, while they were never exceeded for nitrate or phosphate.

6. PAH fingerprint

The PAH fingerprint shows the predominance of high molecular weight PAH species (4-7 rings, from Fluo-Cor in Figure S2) over low molecular weight (2-3 rings, Nap-Phen), indicating that the main PAH sources for this site are pyrogenic . The relatively high variability of Nap and Phen, both typically petrogenic molecules, may correspond to occasional fuel leakage from vehicles (Stogiannidis and Laane, 2015). Phen/A and Fluo/Pyr ratios (2.7±1.0 and 0.83±0.12), indicators commonly used to evaluate PAH sources, were both in the lower range of those previously measured for stormwater and close to ratios calculated for a road determined to be influenced by industrial activity (Brown and Peake, 2006), which may indicate that industrial sources are important for this site, in addition to normal traffic activity.

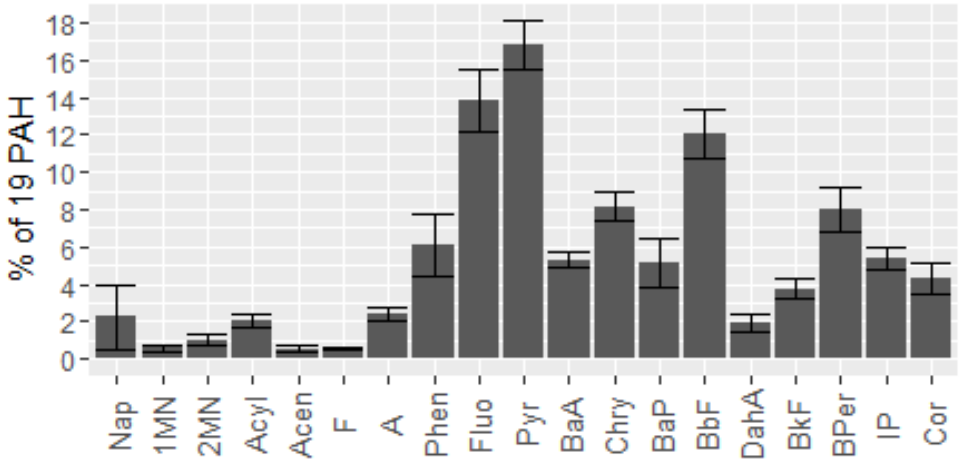

Figure S2: Fingerprint of the 19 PAH molecules (in percent, mean±SD) in road runoff

7. Global parameters

The pH in the VFS drain (median 7.77, Table 4) was consistently lower than that in RR despite the alkaline pH of the filter media, likely due to the biological activity and degradation of organic matter in the soil, resulting in a production of acidifying CO_2. This also occurred to a lesser extent in the BFS, for which outlet pH increased compared to RR during the first period of operation before tending to remain stable or decrease slightly as biological activity was established.

Outlet electrical conductivity (EC) tended to be higher than that in RR. In all seasons, various ions, including Ca and to a lesser extend K and Mg (Table 4) were emitted from the filter media. In winter and into the spring, among the measured ions, EC was dominated by Na from deicing salt applied to the road surface. While high EC was observed at RR immediately following road salt application, EC remained elevated longer at BFS and VFS, which appear to act as temporary reservoirs for salt before it is slowly washed out.

Total concentrations of both KN (the sum of reduced nitrogen species, both organic and ammoniacal) and P were significantly reduced at outlets (Wilcoxon $P<0.01$ except for TP at BFS for which $P<0.05$). Median E_c for TP and TKN (respectively 70 and > 59% for VFS; 41 and 44% for BFS) are similar to previous results demonstrating removal of these species (Davis, 2007; Hunt et al., 2008), while other studies have demonstrated negative E_c (Hunt et al., 2006; Leroy et al., 2016).

Among dissolved species, KN, P, PO_4^{3-} and NO_2^- were rarely quantified, while was significantly lower ($P<0.05$ for both systems). BFS NO_3^- concentrations tended to be higher than in RR, though the difference was not significant (Wilcoxon $P>0.05$) due to an improvement of performance over time.

The sum of all nitrogen species decreased at both outlets (Figure S2). Increases in nitrate at BFS, along with decreases in reduced nitrogen species are indicative of aerobic conditions in the filter, leading to nitrification. E_c for ammonium, nitrite and nitrate are all positively correlated (Spearman $P<0.05$), while no correlation is observed with total TKN E_c. As such, it does not appear that these species are nitrified in BFS at the event scale, but rather that organic nitrogen stored in the filter media is decomposed to ammoniacal nitrogen, which is then nitrified. This hypothesis is compatible with previously reported nitrification half-lives, which generally exceed 13 days even in well-aerated soil (S.R. Buss et al., 2003). The improvement of nitrate removal in BFS over time is likely due to the establishment of the plant and microbial communities (corresponding to increased nitrogen demand).

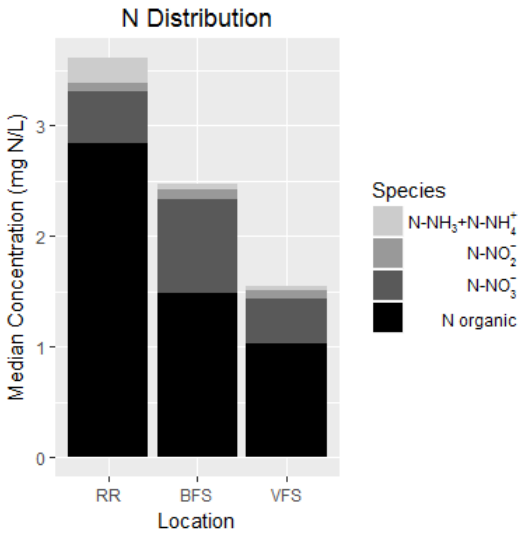

Figure S3: Median total concentrations of all nitrogen species at each sampling location.

8. Percent concentration reductions

Parameter		*Total Concentration Reduction (%)*						*Dissolved Concentration Reduction (%)*					
		VFS	Fsig (%)	*n*	**BFS**	Fsig (%)	*n*	**VFS**	Fsig (%)	*n*	**BFS**	Fsig (%)	*n*
	TSS	94 (82, 98)	100	*13*	92 (11, 95)	100	*11*	-	-	-	-	-	-
	OC	70 (24, 86)	100	*12*	70 (18, 77)	100	*10*	-66 (-183, 32)	8	*13*	-32 (-88, 33)	9	*11*
Nutrients	KN	>59 (-15, 73)	91	*11*	44 (6, 73)	78		-35 (-74, -10)	0	*5*	8 (-25, 23)	0	*4*
	NH_4^+	-			-			64 (-45, 92)	91	*11*	64 (-63, 92)	70	*10*
	NO_3^-	-			-			18 (-413, 76)	55	*11*	-131 (-1825, 57)	11	*9*
	NO_2^-	-			-			27 (-200, 50)	29	*7*	7 (-150, 31)	0	*6*
	P	70 (-62, 88)	75	*12*	41 (-77, 85)	60	*10*	-20 (-50, 29)	0	*6*	-43 (-120, -29)	0	*5*
	PO_4^{3-}	-			-			-	0	*0*	-	0	*0*
Trace Metals	As	68 (53, 87)	100	*10*	20 (-29, 55)	67	*9*	-47 (-239, 52)	22	*9*	-169 (-392, 6)	0	*8*
	Ba	75 (2, 89)	90	*10*	51 (-77, 84)	78	*9*	-94 (-1590, -62)	0	*9*	-223 (-1620,-143)	0	*8*
	Cd	>70 (>10, >82)	90	*10*	>47 (>10, 79)	78	*9*	-	0	*0*	-	0	*0*
	Co	>66 (>44, >84)	100	*8*	>56 (17, 73)	100	*7*	-	0	*0*	-	0	*0*
	Cr	86 (75, 96)	100	*10*	80 (9, 89)	89	*9*	-26 (-160, 41)	11	*9*	-97 (-280, 2)	0	*8*
	Cu	77 (64, 92)	100	*10*	76 (19, 93)	100	*9*	-8 (-206, 42)	22	*9*	21 (-7, 46)	63	*8*
	Mo	45 (-24, 97)	60	*10*	38 (-8, 89)	67	*9*	-85 (-217, 91)	25	*8*	-80 (-189, 84)	17	*6*
	Ni	82 (41, 93)	100	*10*	71 (17, 91)	89	*9*	-10 (-209, 45)	11	*9*	-20 (-104, 46)	13	*8*
	Pb	93 (81, 97)	100	*10*	89 (12, 97)	89	*9*	-22 (-193, 61)	11	*9*	12 (-155, 63)	50	*8*
	Sr	8 (-173, 60)	50	*10*	-39 (-327, 37)	33	*9*	-42 (-455, -5)	0	*9*	-161 (-697, -68)	0	*8*
	V	85 (74, 94)	100	*10*	62 (6, 79)	89	*9*	4 (-82, 55)	44	*9*	-77 (-569, 41)	13	*8*
	Zn	90 (82, 96)	100	*10*	89 (25, 98)	100	*9*	35 (-94, 51)	56	*9*	57 (-74, 76)	88	*8*

Table S3: Summary of global and trace element concentration reductions (E_c for the vegetative filter strip (VFS) and biofiltration swale (BFS). Significant concentration reduction represented by *(P<0.01) or **(P<0.05); significance of concentration increase represented by ° (P<0.01) or °°(P<0.05). F_{sig} refers to the fraction of events for which a concentration reduction was observed, while n is the number of events for which E_c was calculated.

Parameter		*Total Concentration Reduction (%)*						*Dissolved Concentration Reduction (%)*					
		VFS	Fsig (%)	*n*	**BFS**	Fsig (%)	*n*	**VFS**	Fsig (%)	*n*	**BFS**	Fsig (%)	*n*
	TPH	71 (>15, 91)	70	*10*	68 (>8, 81)	60	*10*	-	0	*0*	-	0	*0*
Polycyclic Aromatic Hydrocarbons (PAH)	Nap	74 (>37, 91)	100	*10*	>77 (-1912,87)	80	*10*	19 (4, 33)	0	*2*	-20 (-4120, 33)	0	*5*
	1MN	56 (-3, 70)	70	*9*	>55 (-1858, 69)	78	*9*	13 (9, 17)	0	*2*	0 (-2400, 17)	0	*4*
	2MN	>70 (>16, 87)	80	*10*	>64 (-1182, 85)	80	*10*	9 (9, 41)	0	*3*	-18 (-1900, 41)	0	*4*
	Acyl	>81 (>59, 88)	100	*10*	83 (32, 90)	100	*10*	-	0	*0*	-	0	*0*
	Acen	47 (<-1, 69)	70	*10*	21 (-301, 69)	40	*10*	-	0	*0*	<-415 (-<660,<-160)	0	*4*
	F	54 (2, 75)	70	*10*	>50 (7, 73)	60	*10*	>23 (>0, 25)	0	*3*	0 (-17, >23)	0	*3*
	A	88 (59, 92)	100	*10*	86 (38, 91)	100	*10*	-	0	*0*	-	0	*0*
	Phen	93 (78, 96)	100	*10*	92 (30, 96)	100	*10*	>47 (>9,>90)	73	*11*	>44 (-11,>90)	50	*10*
	Fluo	95 (86, 97)	100	*10*	94 (48, 97)	100	*10*	>33 (>23, 48)	27	*11*	>21 (-292,>47)	20	*10*
	Pyr	95 (91, 98)	100	*10*	94 (42, 95)	100	*10*	>47 (27, >57)	73	*11*	25 (-126, 55)	20	*10*
	BaA	91 (82, 95)	100	*10*	92 (42, 95)	100	*10*	-	0	*0*	-	0	*0*
	Chry	93 (84, 96)	100	*10*	93 (46, 97)	100	*10*	-	0	*0*	-	0	*0*
	BaP	90 (82, 93)	100	*10*	90 (46, 95)	100	*10*	-	0	*0*	-	0	*0*
	BkF	90 (70, 93)	100	*10*	90 (21, 93)	90	*10*	-	0	*0*	-	0	*0*
	BPer	92 (75, 95)	100	*10*	92 (31, 97)	100	*10*	-	0	*0*	-	0	*0*
	IP	90 (69, 95)	100	*10*	90 (24, 96)	100	*10*	-	0	*0*	-	0	*0*
	BbF	93 (79, 98)	100	*10*	92 (36, 97)	100	*10*	-	0	*0*	-	0	*0*
	DahA	83 (62, 86)	100	*10*	>82 (32, 86)	100	*10*	-	0	*0*	-	0	*0*
	Cor	90 (73, 96)	100	*10*	89 (28, 95)	100	*10*	-	0	*0*	-	0	*0*
	Σ16 PAH	91 (81, 95)	-	*10*	91 (81, 95)	-	*10*	-	0	*0*	-	0	*0*

Table S4: Summary of TPH and PAH concentration reductions (E_c for the vegetative filter strip (VFS) and biofiltration swale (BFS). Significant concentration reduction represented by *(P<0.01) or **(P<0.05); significance of concentration increase represented by ° (P<0.01) or °°(P<0.05). F_{sig} refers to the fraction of events for which a concentration reduction was observed, while n is the number of events for which E_c was calculated.

Parameter		Total Concentration Reduction (%)						Dissolved Concentration Reduction (%)					
		VFS	Fsig (%)	*n*	**BFS**	Fsig (%)	*n*	**VFS**	Fsig (%)	*n*	**BFS**	Psig (%)	*n*
	BPA	86 (69, 98)	100	*11*	57 (-57, 79)	78	*9*	79 (49, 93)	100	*12*	43 (-452, 75)	80	*10*
Alkylphenols	OP	93 (51, 97)	100	*11*	76 (-109, 94)	89	*9*	74 (23, 94)	83	*12*	59 (-81, 83)	60	*10*
	OP_1EO	>37 (<-72, 98)	71	*7*	31 (-52, 85)	40	*5*	74 (-174, 94)	60	*5*	47 (4, 85)	50	*4*
	OP_2EO	>72 (>12, 86)	91	*11*	>72 (-252, 84)	67	*9*	49 (25,72)	100	*2*	>49 (>25, >72)	100	*2*
	4-NP	65 (14, 92)	91	*11*	56 (-219, 72)	78	*9*	6 (-125, 59)	25	*12*	4 (-113, 40)	10	*10*
	NP_1EC	32 (0, 88)	64	*11*	-49 (-208, 48)	11	*9*	27 (-3, 88)	42	*12*	-54 (-223, 48)	10	*10*
	NP_1EO	73 (46, 84)	82	*11*	52 (-63, 77)	67	*9*	31 (-106, 59)	17	*6*	32 (-142, 72)	17	*6*
	NP_2EO	38 (-51, 88)	45	*11*	41 (-68, 85)	44	*9*	14 (-89, 70)	33	*12*	24 (-124, 65)	40	*10*
Phthalates	DMP	23 (-231, 72)	9	*11*	23 (-191, 68)	12	*8*	1 (-352, 76)	17	*6*	19 (-276, 76)	20	*5*
	DiBP	41 (-93, 85)	55	*11*	29 (-179, 72)	36	*8*	-23 (-121, 68)	9	*11*	12 (-159, 45)	0	*9*
	DBP	47 (-38, 87)	64	*11*	48 (-988, 87)	62	*8*	8 (-99, 61)	33	*12*	21 (-1831, 92)	44	*9*
	DEHP	69 (-191, 79)	55	*11*	8 (-132, 36)	12	*8*	-5 (-674, 52)	33	*12*	-202 (-754, 62)	11	*9*
	DNP	83 (28, 96)	88	*8*	74 (64, 93)	100	*4*	-7 (-27, 88)	17	*3*	-17	0	*1*

Table S5: Summary of emerging micropollutant concentration reductions (E_c for the vegetative filter strip (VFS) and biofiltration swale (BFS). Significant concentration reduction represented by *(P<0.01) or **(P<0.05); significance of concentration increase represented by ° (P<0.01) or °°(P<0.05). F_{sig} refers to the fraction of events for which a concentration reduction was observed, while n is the number of events for which E_c was calculate

9. Supplementary parameter distributions

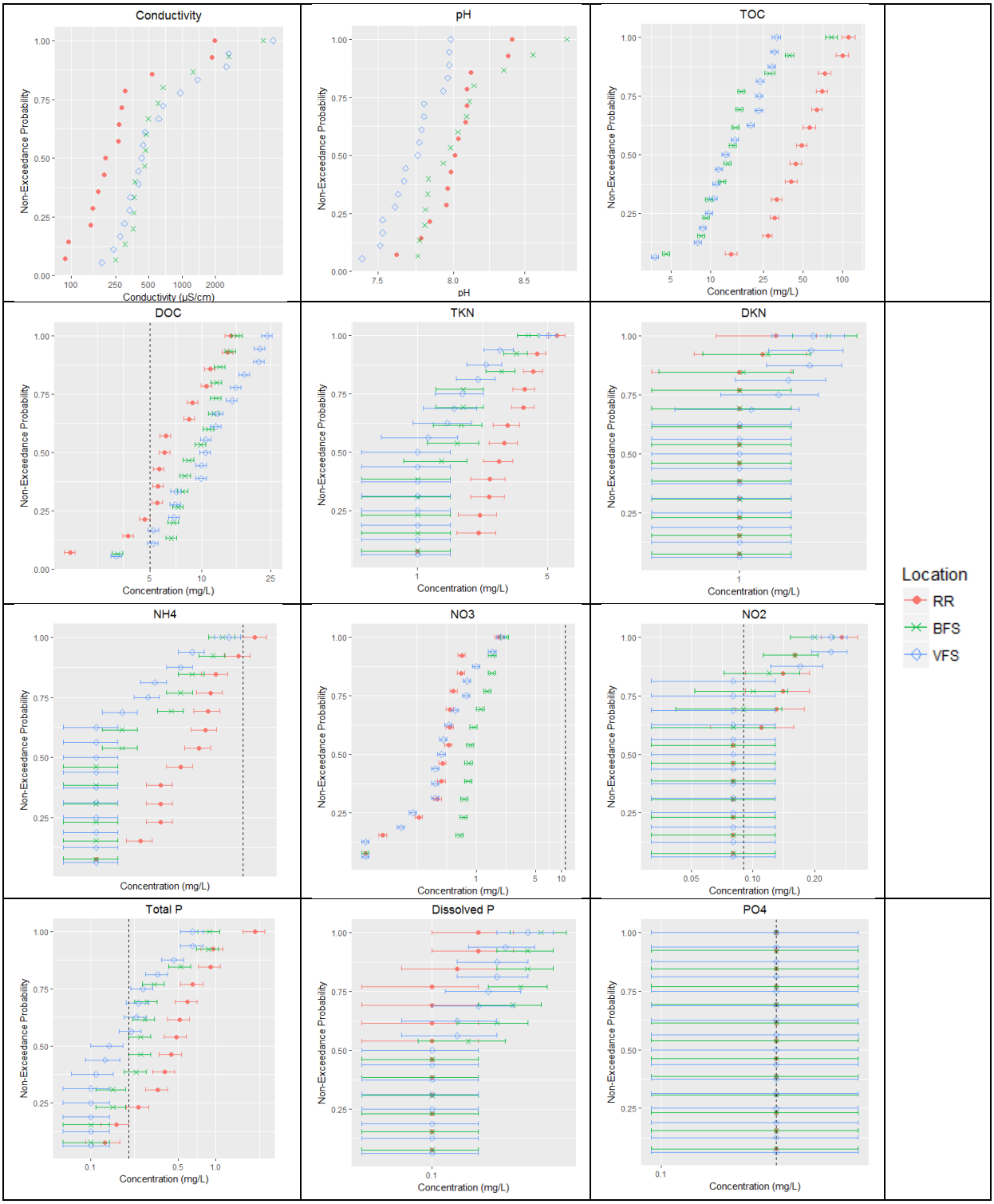

Figure S4: Probability distributions of global parameters in road runoff (RR) and in the drains of the vegetative filter strip (VFS) and the biofiltration swale (BFS). Error bars represent analytical uncertainty while the dotted black line represents the EQS.

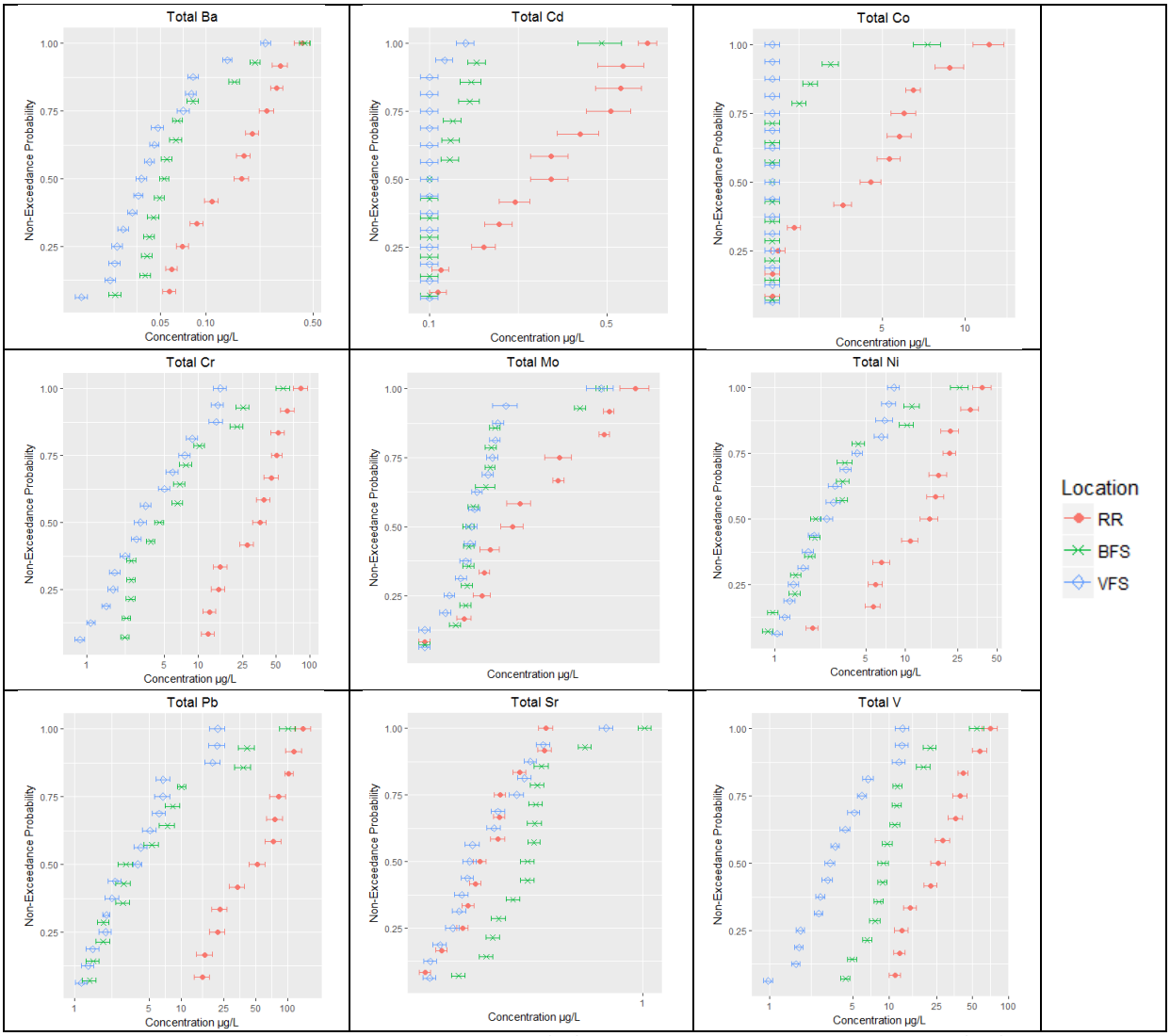

Figure S5: Probability distributions of total trace elements in road runoff (RR) and in the drains of the vegetative filter strip (VFS) and the biofiltration swale (BFS). Error bars represent analytical uncertainty while the dotted black line represents the EQS.

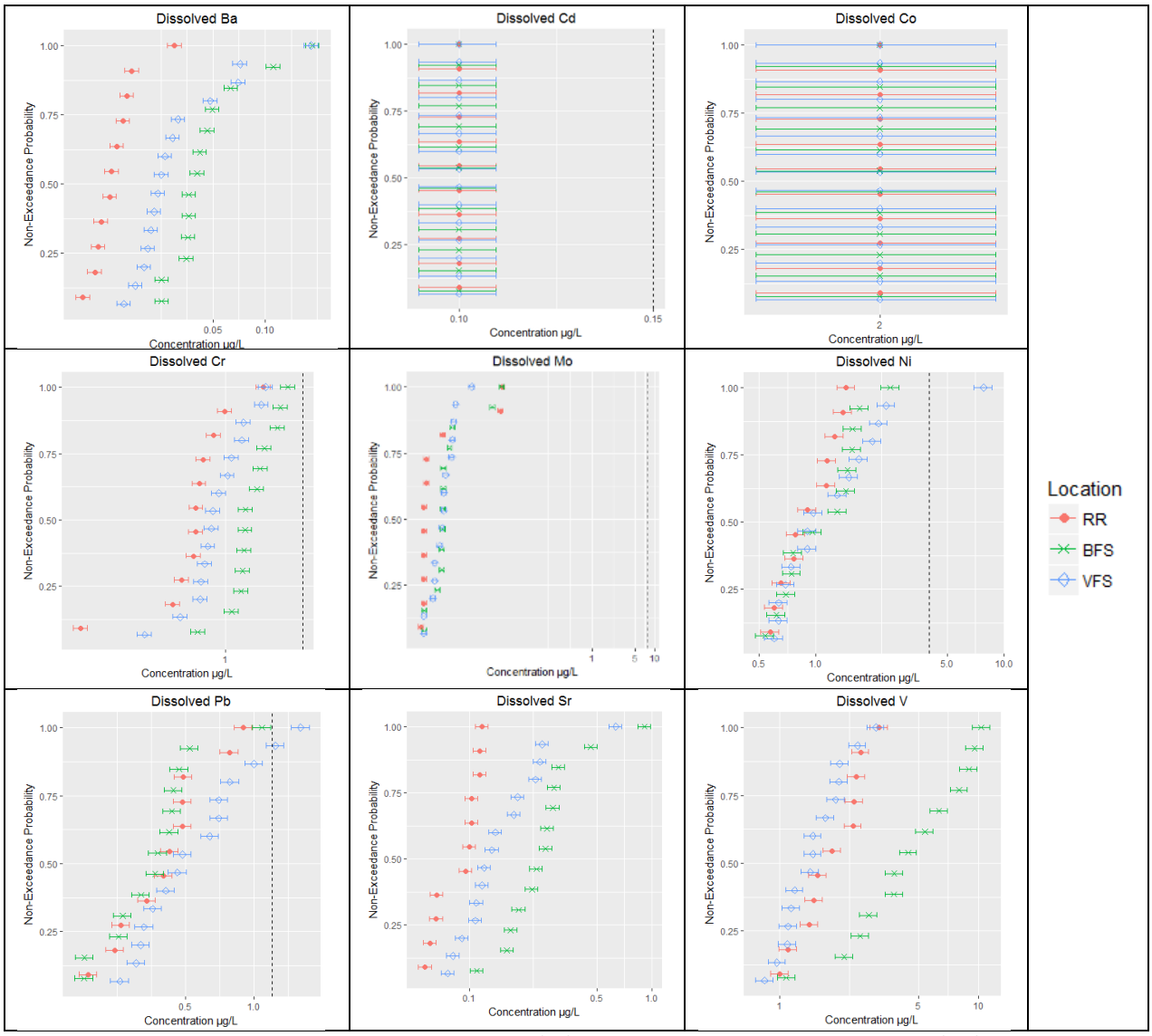

Figure S6: Probability distributions of total trace elements in road runoff (RR) and in the drains of the vegetative filter strip (VFS) and the biofiltration swale (BFS). Error bars represent analytical uncertainty while the dotted black line represents the EQS.

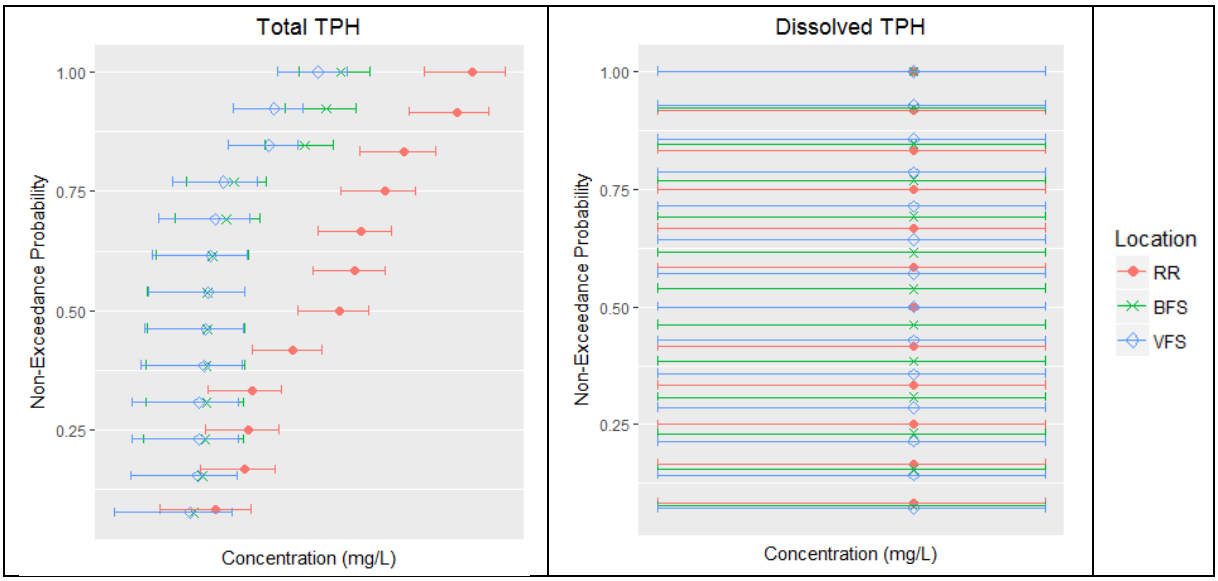

Figure S7: Probability distributions of total and dissolved total petroleum hydrocarbons (TPH) in road runoff (RR) and in the drains of the vegetative filter strip (VFS) and the biofiltration swale (BFS). Error bars represent analytical uncertainty while the dotted black line represents the EQS.

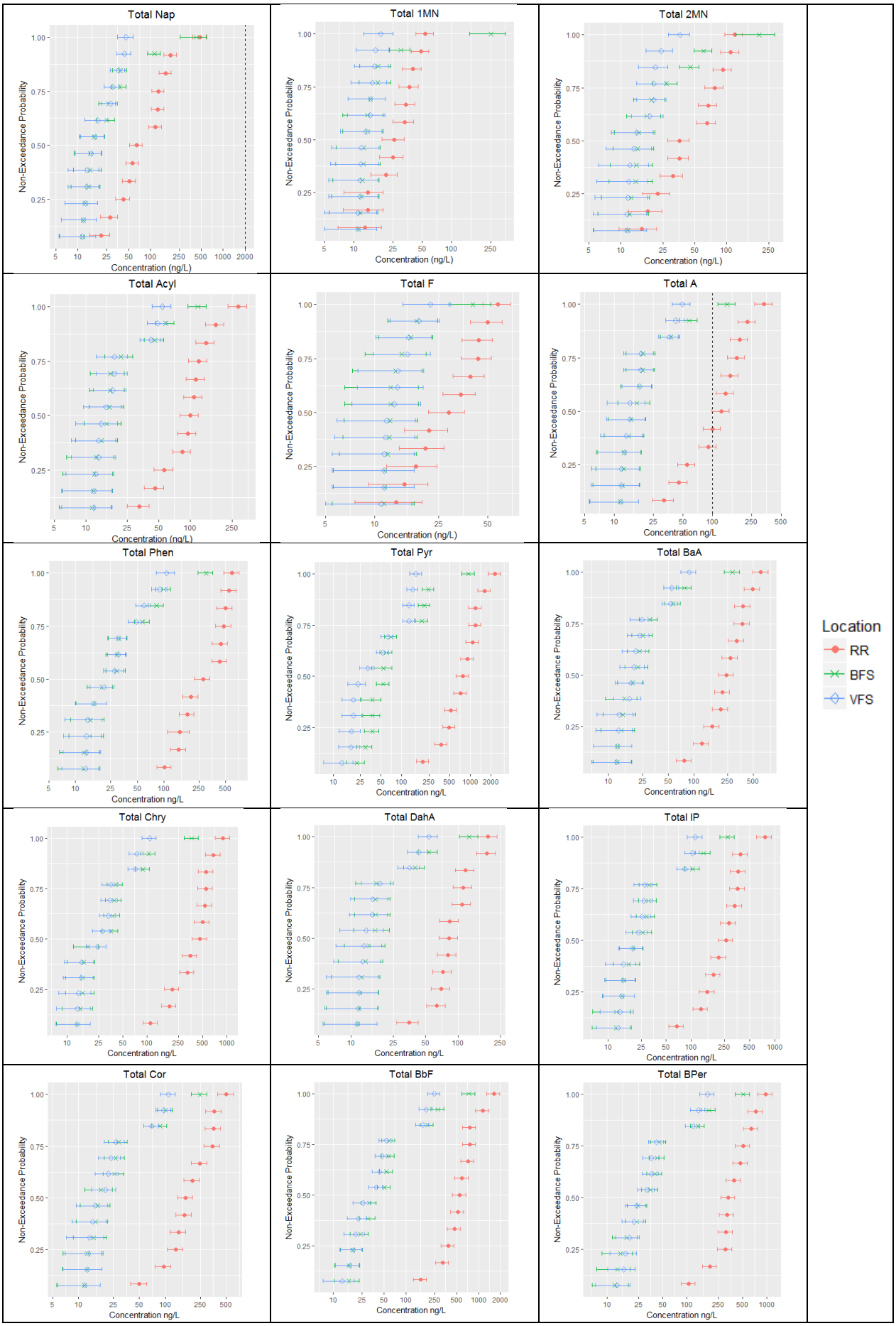

Figure S8: Probability distributions of total polycyclyic aromatic hydrocarbons (PAH) in road runoff (RR) and in the drains of the vegetative filter strip (VFS) and the biofiltration swale (BFS). Error bars represent analytical uncertainty while the dotted black line represents the EQS.

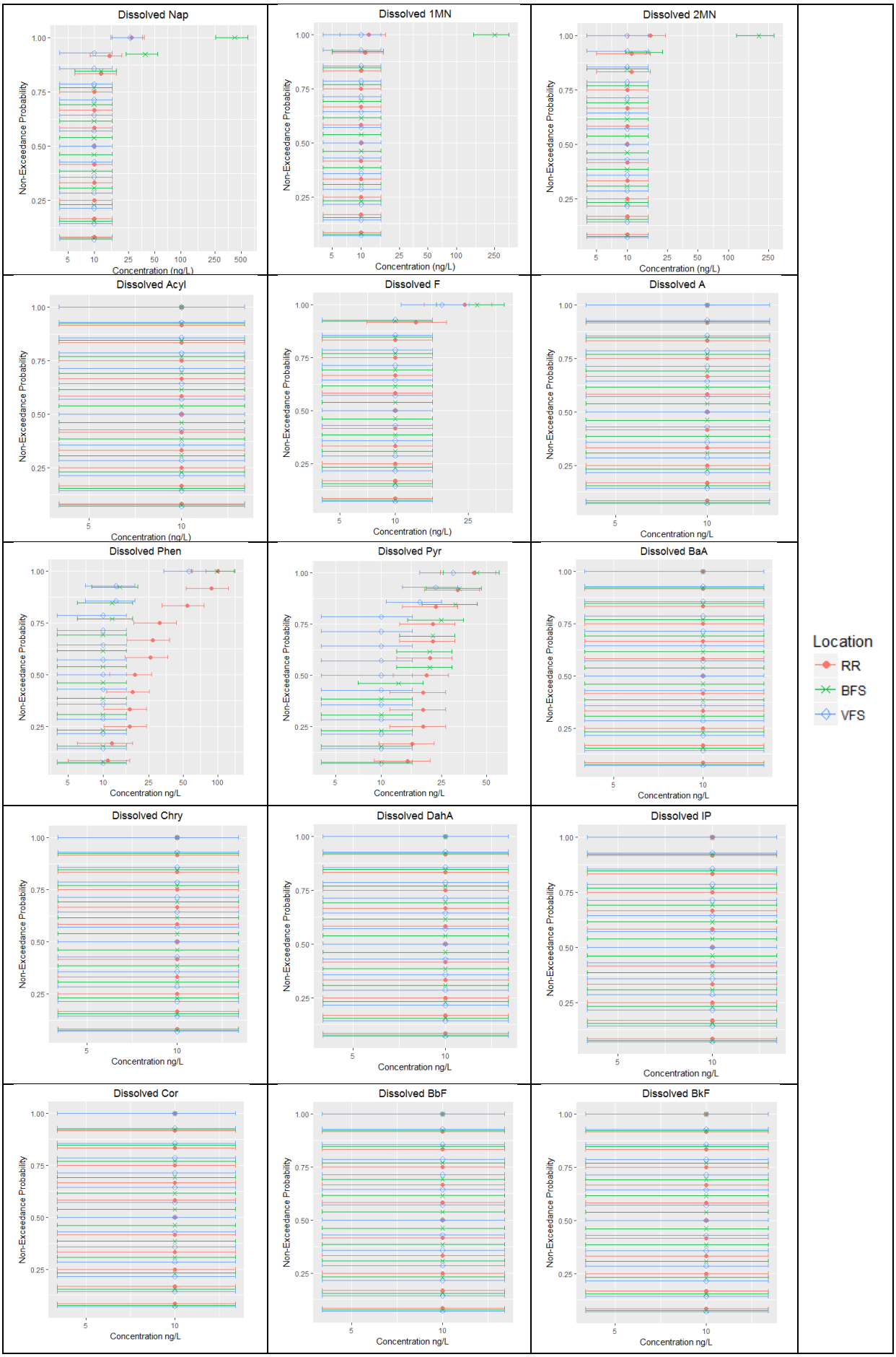

Figure S9: Probability distributions of dissolved polycyclic aromatic hydrocarbons (PAH) in road runoff (RR) and in the drains of the vegetative filter strip (VFS) and the biofiltration swale (BFS). Error bars represent analytical uncertainty while the dotted black line represents the EQS.

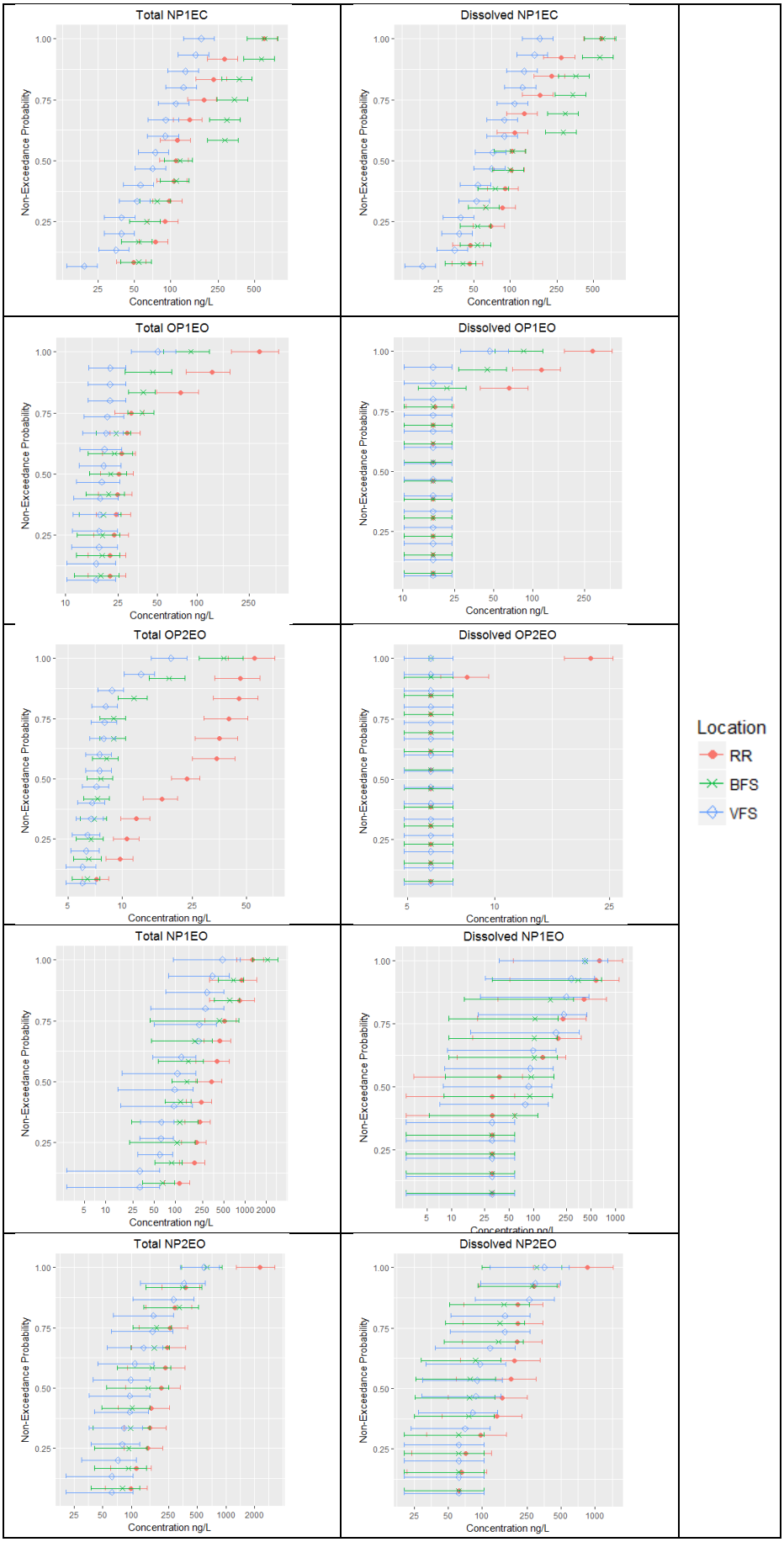

Figure S10: Probability distributions of total and dissolved alkylphenols in road runoff (RR) and in the drains of the vegetative filter strip (VFS) and the biofiltration swale (BFS). Error bars represent analytical uncertainty while the dotted black line represents the EQS.

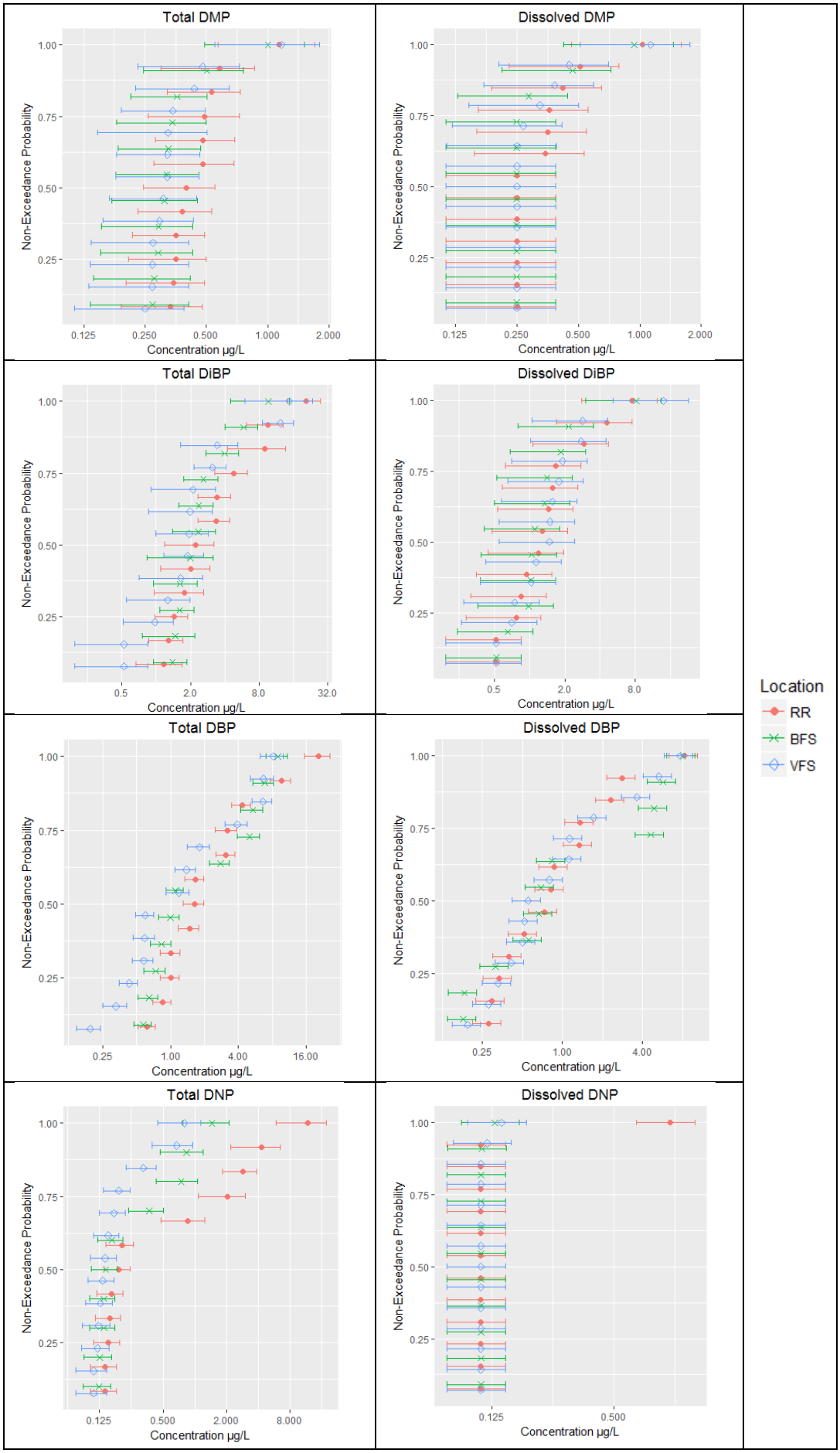
Total DMP
Dissolved DMP
Total DiBP
Dissolved DiBP
Total DBP
Dissolved DBP
Total DNP
Dissolved DNP
Non-Exceedance Probability
Concentration µg/L
Location
RR
BFS
VFS

Figure S11: Probability distributions of total and dissolved phthalates in road runoff (RR) and in the drains of the vegetative filter strip (VFS) and the biofiltration swale (BFS). Error bars represent analytical uncertainty while the dotted black line represents the EQS.

10. Selected Pollutant Time Series

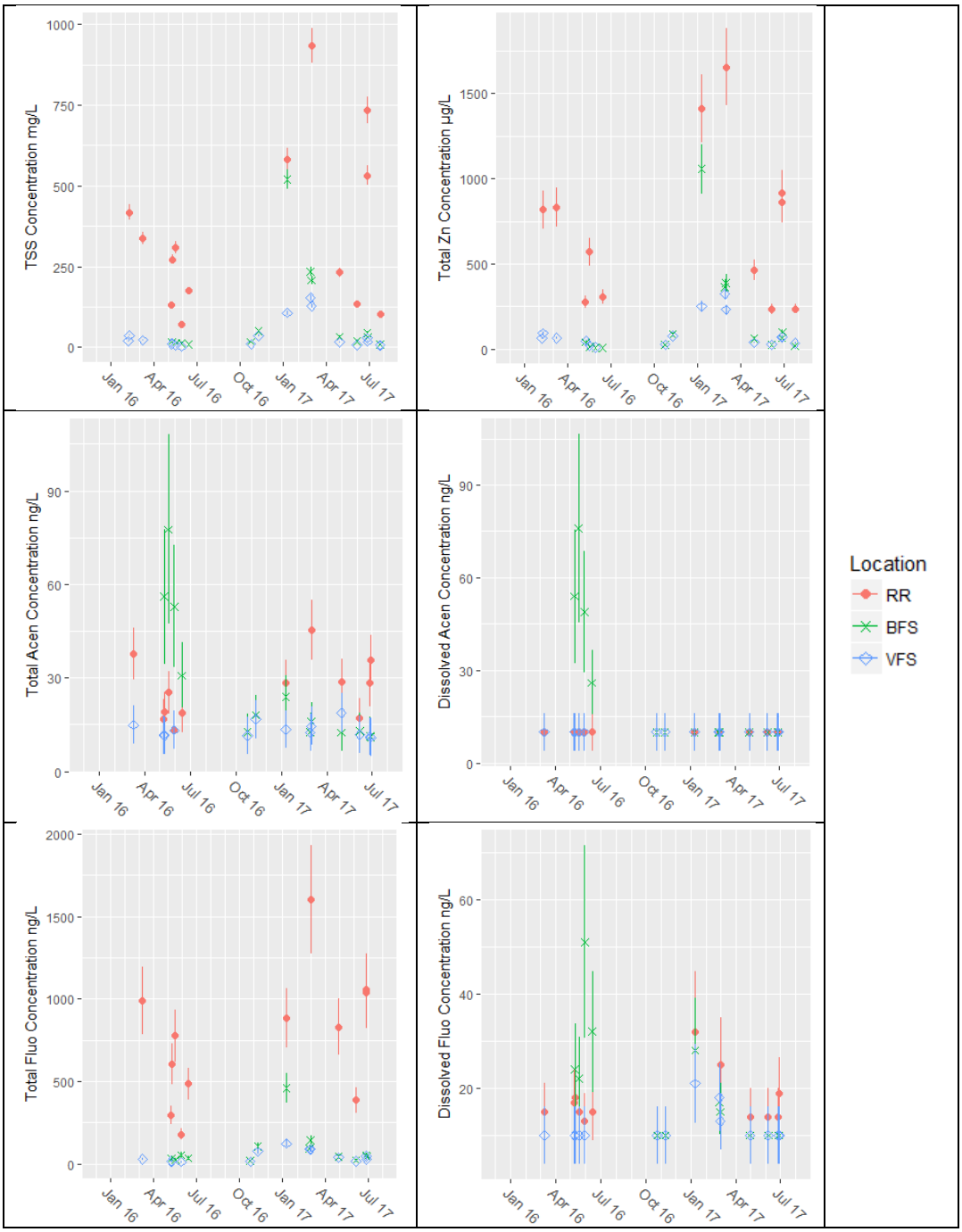

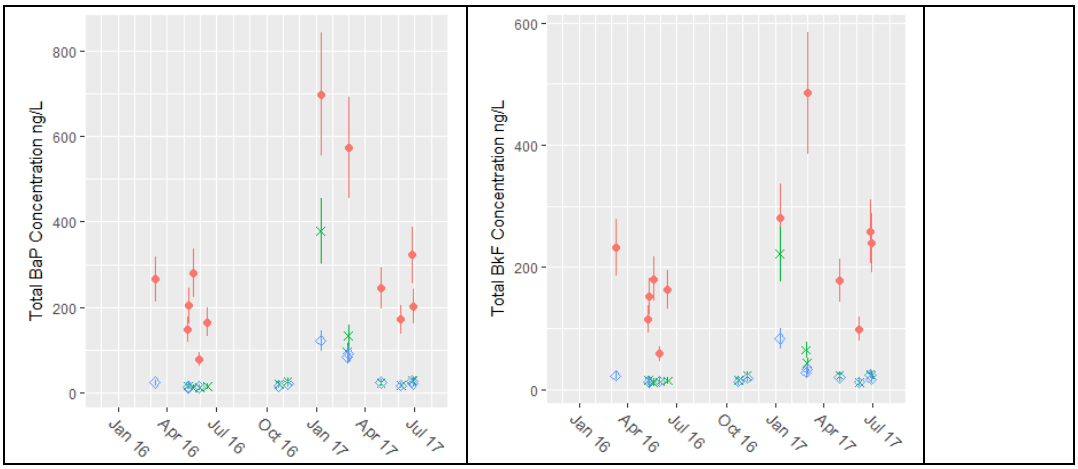

Figure S12: Time series of pollutant concentrations in road runoff (RR), the biofiltration swale (BFS) and the vegetative filter strip (VFS)*

11. Relationship between hydrobicity and partitioning

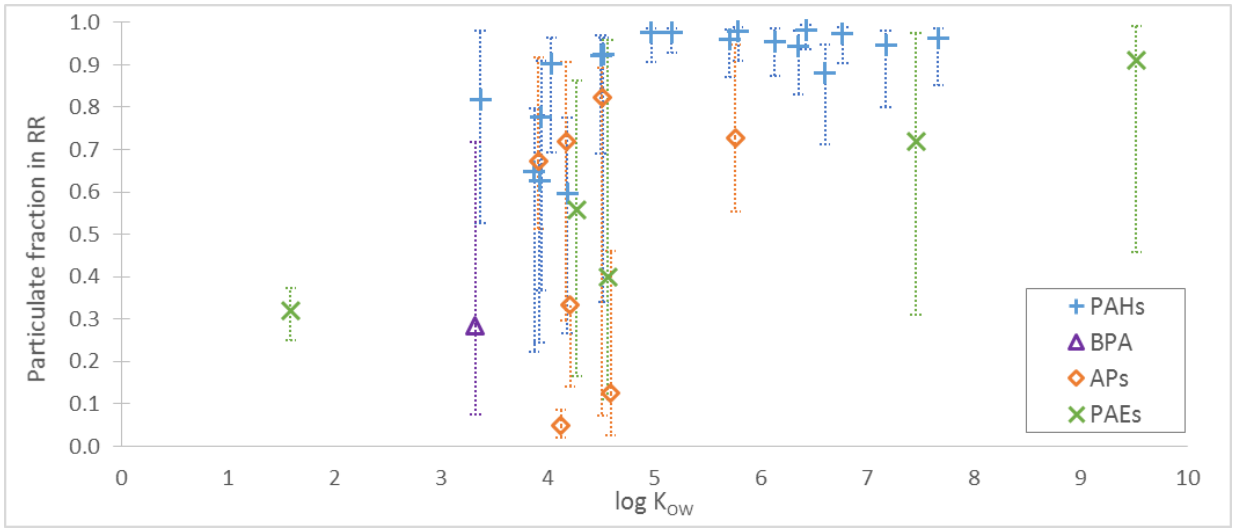

Figure S13: Particulate fraction of organic micropollutants in RR according to Kow. Points represent median particulate fractions, while error bars represent minimal and maximal observed values.

(a)

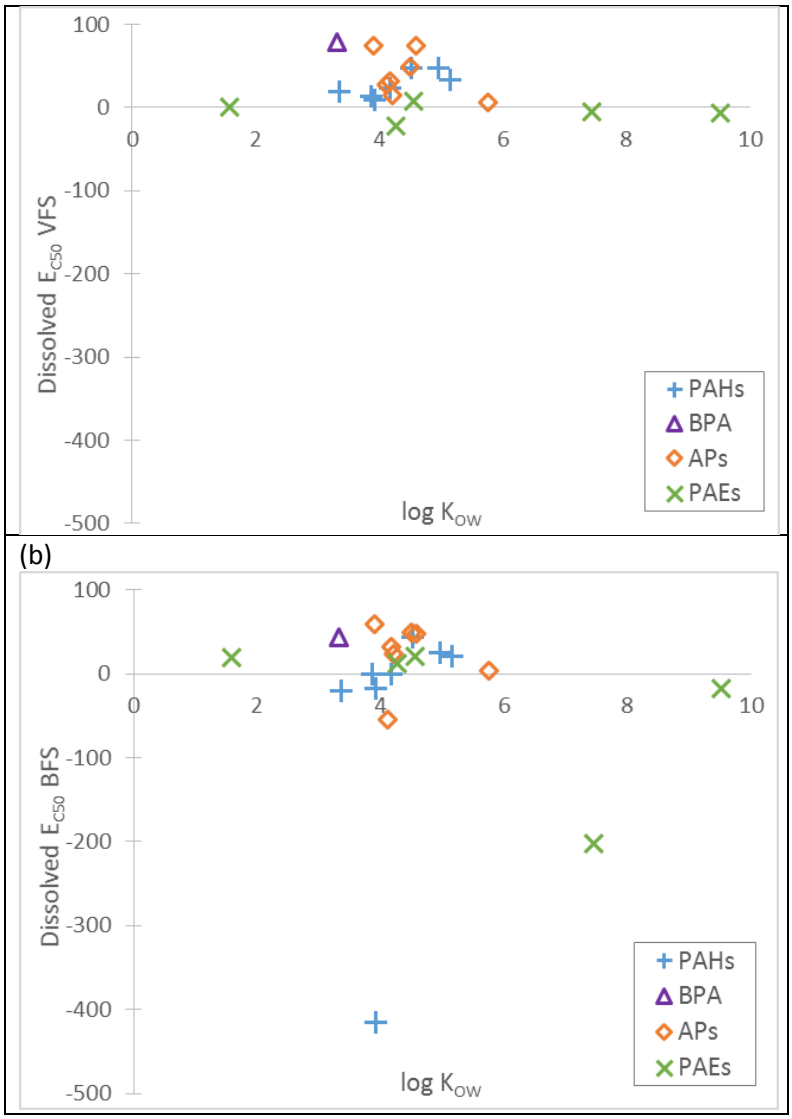

Figure S14: Relationships between dissolved Ec50 and Koc in (e) VFS and (f) BFS.